Design and Performance of Asymmetric Waveguide Nitride Laser Diodes

D. P. Bour, M. Kneissl, C. G. Van de Walle, G. A. Evans, L. T. Romano, J. Northrup, M. Teepe, R. Wood, T. Schmidt, S. Schoffberger, and N. M. Johnson

Abstract—**We describe the design and performance characteristics of an asymmetric waveguide nitride laser diode structure, in which the *p*-cladding layer is placed immediately over the multiple-quantum-well (MQW) active region. Its close proximity to the active region enables it to serve not only as a cladding layer, but also as a potential barrier that confines injected electrons. This structure represents a departure from conventional nitride laser diode structures, where electron confinement is provided by a separate high-aluminum-content AlGaN tunnel barrier layer placed over the MQW active region. The optical confinement factor (Γ) remains comparable to that of the conventional structure, in spite of the QW's displacement from the center of the waveguide. Room-temperature CW operation was achieved with this structure.**

Index Terms—**CVD, group-III nitrides, InGaN quantum well, quantum-well lasers, semiconductor epitaxial layers, semiconductor lasers.**

I. Introduction

SINCE their initial demonstration in 1995, nitride laser diodes have undergone rapid development, led by Nakamura and his coworkers at Nichia Chemical Industries, Japan [1]–[18]. When focused in an optical system, their short emission wavelength (400 nm band) translates into a small spot size for high-density optical storage or high-resolution laser printing. Furthermore, compact violet-blue lasers may also be applied to spectroscopy and projection displays, and they may also be used to generate other colors or white light by exciting phosphors.

Common features among the best nitride laser diodes demonstrated to date include an InGaN multiple-quantum-well (MQW) active region within a separate confinement heterostructure (SCH), and AlGaN cladding layers. In addition, a high-aluminum-content p-type AlGaN:Mg layer is also grown immediately over the QW's [1]–[10]. This layer serves to protect and stabilize the InGaN QW surface. It also comprises a high-bandgap tunnel barrier layer that prevents the leakage of electrons which have been injected into the MQW active region. Thus, this layer serves a critical role in achieving optimum performance in nitride laser diodes.

Manuscript received June 1, 1999; revised September 16, 1999. This work was supported in part by the Defense Advanced Projects Agency (DARPA) under Contract MDA972-96-0014.

D. P. Bour, M. Kneissl, C. G. Van de Walle, L. T. Romano, J. Northrup, M. Teepe, R. Wood, T. Schmidt, S. Schoffberger, and N. M. Johnson are with the Electronic Materials Laboratory, Xerox Palo Alto Research Center, Palo Alto, CA 94304 USA.

G. A. Evans is with the School of Engineering and Applied Science, Southern Methodist University, Dallas, TX 75275 USA.

Publisher Item Identifier S 0018-9197(00)00957-X.

In this paper, we describe the design considerations and performance characteristics of an asymmetric waveguide nitride laser structure. It eliminates the high-aluminum tunnel barrier layer and instead uses the p-cladding layer to confine injected electrons. In this respect, this nitride structure is functionally similar to more common arsenide and phosphide lasers. However, the short minority-electron diffusion length in nitride materials dictates that the confining barrier (in this case the p-cladding layer) be placed in very close proximity to the QW's [20]. Despite the resultant asymmetric waveguide, in which the QW's are displaced from the center of the waveguide, this structure still achieves an optical confinement factor comparable to that of the conventional nitride laser structure.

II. Asymmetric Waveguide Structure

For laser diodes incorporated into printing and optical storage systems, reliable, low-threshold operation is a basic requirement. Among the difficulties associated with achieving low-threshold operation is the confinement of injected charge carriers. Often in laser diodes, for instance, the injected electrons are not adequately confined, and they leak away from the QW active region to recombine with the majority holes in the p-cladding layer. Since leaked electrons do not populate the active region and do not contribute to stimulated emission, the threshold current is increased and the internal quantum efficiency is reduced by leakage. Notably, in the nitride laser structures pioneered by Nakamura *et al.*, a thin, high-bandgap, p-type AlGaN layer is placed immediately above the active region [1]–[10]. Placing such a thermally stable material over the InGaN MQW may preserve this critical surface by suppressing dissociation, thereby preserving the structural and optoelectronic quality of the active region [2]. This layer may also play a secondary role, however, by confining injected electrons.

The function of this tunnel barrier layer is illustrated in Fig. 1, a simplified band diagram which shows how the p-type high-bandgap AlGaN layer presents a strong confinement barrier for electrons injected into the QW's. In this crude flat-band construction, we have ignored the piezoelectric fields, the electric fields associated with nonuniformities in the injected carrier distribution, and the fields required to support charge injection into the active region. Typically, in the nitride laser diode structures currently reported, a 200-Å layer of (p-type) $Al_{0.2}Ga_{0.8}N$:Mg prevents energetic electrons (those which have enough energy to escape from the wells) from diffusing or drifting into the p-type material, where they would rapidly recombine with the

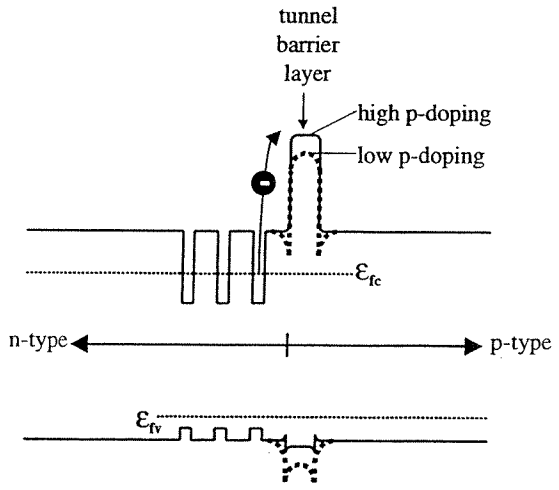

Fig. 1. Simplified band diagram illustrating how a high-bandgap AlGaN:Mg layer placed over the InGaN MQW in a nitride laser structure serves as a tunnel barrier. In this schematic, the ideal case where the p-doping is high (solid curve) is compared to the more realistic case where the p-doping is limited by Mg acceptor solubility and high acceptor activation energy (dashed line).

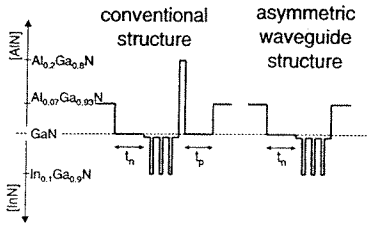

Fig. 2. Schematic composition profiles of the conventional nitride laser structure (left, with the QW's located near the center of a GaN waveguide, and with an AlGaN layer over the QW's), and the asymmetric structure (right, where the QW's are adjacent to the p-cladding layer).

available holes. With the electron leakage current reduced in this manner, the laser threshold current is lower and also less temperature-sensitive. Also, the internal quantum efficiency remains high.

Among the challenges in the successful operation of these conventional nitride laser diode structures is p-type doping of the high-bandgap AlGaN tunnel barrier layer. In particular, the acceptor activation energy increases by approximately 3 meV for every 1% increase in AlN alloy content, so that the hole concentration in an $Al_{0.2}Ga_{0.8}N$:Mg layer is diminished by at least one order of magnitude compared to that of a GaN:Mg film with the same acceptor concentration [21]. If the hole concentration in this barrier layer is not sufficiently high, its ability to block leaked electrons is compromised, because the effective barrier height decreases for lower p-type doping concentration, as shown in Fig. 1. Furthermore, when the p-type doping in this layer is low, a barrier-to-hole injection is also created in the valence band edge, resulting in an apparent increase in the diode's resistance. Finally, the parasitic gas-phase reaction between trimethylaluminum and ammonia can make the growth of high-aluminum-content AlGaN films problematic [22]. Consequently, these issues associated with AlGaN growth and p-type doping make it difficult to realize an ideal tunnel barrier layer.

Such high-bandgap tunnel barriers are not routinely used in other laser diode material systems. Instead, for example, in AlGaInP red lasers, the p-cladding layer serves to confine injected electrons [23]–[25]. In this case, the minority electron diffusion lengths are sufficiently large that such a confinement scheme is effective. Specifically, the minority electron diffusion length is on the order of 1 μm, many times greater than the typical 100–200-nm displacement between the QW active region and the p-cladding layer. Therefore, the p-cladding layer represents an effective barrier, because electrons can interact with the barrier created by the p-cladding layer before having an opportunity to recombine.

Suppressing electron leakage is, unfortunately, not so straightforward for nitride lasers. In particular, the minority carrier diffusion lengths in nitrides are on the order of only $\sim$100 nm, many times shorter than in arsenide and phosphide laser materials [20]. Consequently, in nitride lasers, when the wavegide thicknesses are optimized for the highest optical confinement factor, the p-cladding layer may lie several diffusion lengths away from the MQW active region. Therefore, injected electrons are not appreciably confined by the p-cladding layer. This situation contrasts sharply with red and infrared (IR) lasers, where the waveguide thickness is a mere fraction of the minority carrier diffusion length, so that the cladding layer can effectively suppress leakage. Thus, in nitride lasers, a separate tunnel barrier layer placed in very close proximity to the MQW active region is required to prevent electron leakage.

It is thus apparent that, in nitride lasers, the p-cladding layer might also be utilized to confine injected electrons, but only if it is placed in close proximity to the MQW active region (within much less than a minority electron diffusion length). This presents a dilemma, however, since the InGaN QW's, along with the overlying AlGaN tunnel barrier layer, are typically placed at the core of a GaN waveguide region, as shown in Fig. 2 for a conventional nitride laser diode structure. The waveguide thicknesses (t_n and t_p) are independently adjusted to maximize the spatial overlap between the optical mode and the optical gain (optical confinement factor Γ). In nitride lasers, the optimum thickness for each half-waveguide is $\sim$0.1 μm, corresponding to $\geq$1 electron diffusion length. Therefore, in this conventional nitride structure, the p-cladding layer is beyond the horizon of injected electrons and the additional AlGaN tunnel barrier layer supplies the requisite confinement.

To achieve sufficient electron confinement without the AlGaN tunnel barrier, an asymmetric waveguide structure may be employed. An asymmetric waveguide structure results when the MQW is located immediately adjacent to the p-cladding layer, displaced from the center of the waveguide. This asymmetric waveguide structure is shown schematically in Fig. 2, in comparison with the conventional nitride laser structure. Waveguide modeling of such an asymmetric nitride laser structure, described below, reveals that a high optical confinement factor can still be realized, in spite of the off-center placement of the QW's. These simulations indicate that nitride laser diodes are relatively insensitive to such gross asymmetries, because their transverse waveguiding is rather weak, with much of the mode spreading evanescently into the cladding layers. Indeed, the refractive index difference between the GaN waveguide region and the AlGaN cladding layers is only $\Delta n \sim 0.05$, nearly one order of magnitude less than the index difference

TABLE I
LIST OF INDEX AND THICKNESS VALUES FOR INDIVIDUAL LAYERS COMPRISING THE CONVENTIONAL NITRIDE LASER AND THE ASYMMETRIC WAVEGUIDE STRUCTURE

layer	conventional structure n	conventional structure thickness	asymmetric waveguide n	asymmetric waveguide thickness
Sapphire			1.78	semi-∞
GaN:Si			2.51	4 μm
$Al_{0.07}Ga_{0.93}N$:Si cladding layer	2.46	semi-∞	2.46	1 μm or semi-∞
GaN:Si waveguide	2.51	$t_{n,opt}$ ~ 90 nm	2.51	t_n
$In_{0.02}Ga_{0.98}N$:Si barrier	2.52	6 nm	2.52	6 nm
$In_{0.1}Ga_{0.9}N$ QW	2.56	3.5 nm	2.56	3.5 nm
$In_{0.02}Ga_{0.98}N$:Si barrier	2.52	6 nm	2.52	6 nm
$In_{0.1}Ga_{0.9}N$ QW	2.56	3.5 nm	2.56	3.5 nm
$In_{0.02}Ga_{0.98}N$:Si barrier	2.52	6 nm	2.52	6 nm
$In_{0.1}Ga_{0.9}N$ QW	2.56	3.5 nm	2.56	3.5 nm
$In_{0.02}Ga_{0.98}N$:Si barrier	2.52	6 nm	2.52	6 nm
$In_{0.1}Ga_{0.9}N$ QW	2.56	3.5 nm	2.56	3.5 nm
$In_{0.02}Ga_{0.98}N$:Si barrier	2.52	6 nm	2.52	6 nm
$In_{0.1}Ga_{0.9}N$ QW	2.56	3.5 nm	2.56	3.5 nm
$In_{0.02}Ga_{0.98}N$:Si barrier	2.52	6 nm	2.52	6 nm
$Al_{0.2}Ga_{0.8}N$:Mg capping layer	2.37	20 nm	—	---
GaN:Mg waveguide	2.51	$t_{p,opt}$ ~ 85 nm	—	---
$Al_{0.07}Ga_{0.93}N$:Mg cladding layer	2.46	semi-∞	2.46	semi-∞

that can be achieved in AlGaAs lasers. This weaker transverse waveguiding translates into a less-strongly-peaked waveguide mode, and the optical confinement factor is, therefore, less sensitive to any waveguide asymmetry.

A primary advantage of the asymmetric waveguide structure is that it eliminates the need to include a p-type, very-high-bandgap, high-aluminum-content tunnel barrier layer. The growth of such a conventional blocking layer presents practical difficulties including p-type doping and parasitic gas-phase reactions during metal–organic chemical vapor deposition (MOCVD) growth, which can make the growth of such highly p-type high-aluminum-content alloys both difficult and irreproducible. In contrast, the preparation of lower aluminum-content alloys, such as the $Al_{0.07}Ga_{0.93}N$:Mg used for the cladding layers, is more straightforward and reproducible [22]. Since this structure utilizes a lower bandgap alloy to confine injected electrons ($Al_{0.07}Ga_{0.93}N$ of the p-cladding layer instead of $Al_{0.2}Ga_{0.8}N$), however, the electron confinement barrier is accordingly lower. Consequently, electron leakage may not be as well suppressed, in which case the threshold current would become higher and more temperature-sensitive (ie., a low characteristic temperature T_o). Although this difference is perhaps partially offset by the limited p-doping for high-aluminum-content alloys, it is still possible to achieve a bandgap energy difference between the active region and cladding layer of ~500 meV. Moreover, in the asymmetric waveguide structure, the AlGaN cladding layer deposited immediately over the MQW may also preserve the InGaN MQW, much like the AlGaN tunnel barrier layer in a conventional structure [2].

III. Optical Mode Analysis

The transverse optical mode analysis was performed using MODEIG dielectric waveguide simulation software.[1] The mode profiles and optical confinement factors were compared for conventional and asymmetric waveguide structures, each comprising a 5-QW $In_{0.1}Ga_{0.9}N/In_{0.02}Ga_{0.98}N$ 35/60 Å active region and $Al_{0.07}Ga_{0.93}N$ cladding layers, as shown in Fig. 2. The 5-QW active region structure was chosen because it represents the structure with which we have achieved lowest threshold current. It corresponds to the experimental structure whose performance is described below. The refractive index values and layer thicknesses are tabulated in Table I for each of these structures. For all simulations described here, the wavelength was taken to be 400 nm.

For simplicity of analysis, it is most convenient to assume that the $Al_{0.07}Ga_{0.93}N$ cladding layers have semi-infinite thickness. This represents the ideal case; in reality, the cladding layer thickness is limited by cracking. For bulk $Al_{0.07}Ga_{0.93}N$ cladding layers, the cracking threshold is approximately 600 nm, while for superlattice cladding layers of the same average composition the cracking threshold may be increased beyond 1 μm [5]–[10]. Consequently, for bulk cladding layers, the evanescent tail of the optical mode may not decay sufficiently, and some fraction of the mode propagates in the thick n-type GaN that underlies the laser heterostructure (serving as an n-lateral-contact layer). Thus, while their weak transverse guiding makes nitride lasers

[1]PC and Macintosh versions of MODEIG may be downloaded from the website. Available HTTP: http://www.seas.smu.edu/modeig

somewhat insensitive to waveguide asymmetries, it also contributes to incomplete confinement of the mode.

Such mode spreading is commonly observed in nitride lasers with bulk AlGaN cladding layers [3], [4], [26], [27]. In this situation, the lasing mode represents a high-order mode associated with the entire epitaxial layer structure (~5-μm thickness). Although the mode is still largely concentrated within the intended waveguide, the transverse beam far-field profile exhibits multiple interference fringes, indicating operation in a high-order mode. Likewise, the optical confinement factor is slightly reduced by this mode spreading. Even for a 500-nm cladding layer, however, the fraction of the mode propagating outside the waveguide is usually fairly small, such that Γ is reduced by only a small amount. For $\geq$1-μm—thick superlattice cladding layers, the Γ value (and the beam profile) can be essentially indistinguishable from the ideal case [8]. Therefore, the comparisons here are largely based on analysis of structures with semi-infinite cladding layers. This assumption greatly simplifies the waveguide analysis, since the number of mode solutions is much less than if the full epitaxial structure were considered. Nevertheless, this approximation was checked by comparing the results for asymmetric waveguide structures containing either semi-infinite or 1.0-μm-thick n-cladding layers.

Finally, in our analysis, all the layers comprising the structures were assumed to be transparent. Neither the QW gain nor the modal loss (α) associated with the p-metal contact was considered. In separate calculations, however, the effect of an absorbing p-metal (30 nm Ti or Ni + 500 nm Au) was considered. While the modal loss was a strong function of the p-cladding layer thickness, it became negligible ($\alpha_{\text{metal}} < 5$ cm^{-1}, compared to the total distributed loss of 40–60 cm^{-1}), for p-cladding thicknesses $\geq$0.5 μm (and with the GaN:Mg cap layer 0.1 μm). For either Ni-Au or Ti-Au p-contact metals, the modal absorption losses were similar. Although this modal loss exhibited a strong dependence on the p-clad thickness, however, the optical confinement factor was not significantly influenced by the presence of an absorbing metal contact. This is not surprising, since the real part of the Ni, Ti, or Au metal's complex refractive index is low compared to that of the semiconductor; therefore, the mode tends to decay abruptly at the semiconductor–metal interface, as it also would at a semiconductor–air interface.

The optical mode intensity profile and corresponding refractive index profile for an optimized conventional nitride laser structure are shown in Fig. 3. By separately adjusting the n- and p-waveguide layer thicknesses, optimum values were determined. The optimum t_n and t_p values are slightly different because the 200-Å $Al_{0.2}Ga_{0.8}N$ layer over the QW's introduces a significant asymmetry that distorts the mode profile. For these optimal values, the optical confinement factor reaches its maximum value of about 5.2% (summed over all five QW's).

In this conventional structure, the presence of the AlGaN layer over the QW's has an appreciable effect on the mode profile, as is apparent in Fig. 3. Such a low-index layer inserted next to the QW's tends to distort the mode, reducing the total optical confinement factor (Γ_{total}) from a value of about 6.1% (for an optimized, symmetric structure with the AlGaN tunnel barrier layer removed) to only 5.2%. Thus, this AlGaN layer represents a tradeoff between optical and electrical confinement in nitride laser structures.

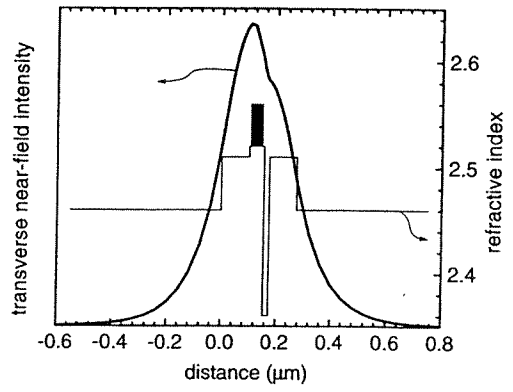

Fig. 3. Optical mode intensity profile and refractive index profile for an optimized, conventional nitride laser diode structure.

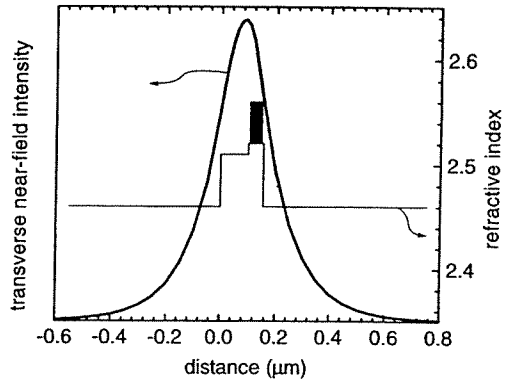

Fig. 4. Optical mode intensity profile and refractive index profile for an optimized, asymmetric waveguide nitride laser diode structure.

The refractive index profile and corresponding optical mode profile are shown in Fig. 4 for the asymmetric structure, for which the high-aluminum-content tunnel barrier layer is eliminated and the p-cladding layer is deposited immediately above the MQW to confine electrons. It is clear from these profiles that, in the asymmetric structure, the QW's are severely displaced from the peak of the mode, compared to the conventional structure. This asymmetry alone produces an appreciable reduction in the maximum Γ_{total} value, from 6.1% (for an optimized, symmetric structure with no AlGaN tunnel barrier) to 5.3%. Nevertheless, the maximum optical confinement factor, obtained when the n-waveguide thickness $t_n = 90$ nm, still slightly exceeds the maximum value obtained by the conventional structure, shown for reference by line 3 in Fig. 5. This is so primarily because the transverse mode in nitride lasers is relatively weakly confined; therefore, the Γ value is not so seriously degraded by the highly asymmetric placement of the QW's. In addition, the distortion caused by the low-index AlGaN layer, placed within the waveguide of the conventional structure, is also responsible for the comparable Γ values. Note that both optimized structures still have Γ_{total} values appreciably lower than could be achieved if the AlGaN overlayer were eliminated from the conventional structure ($\Gamma_{\text{total}} \sim 6.1\%$), shown by line 4 in Fig. 5.

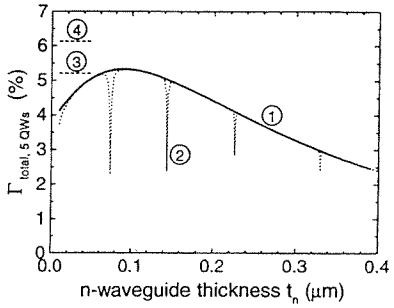

Fig. 5. Total optical confinement factor (Γ_{total}) for the asymmetric waveguide structure, as a function of the n-waveguide thickness t_n: curve 1 (solid) is calculated assuming a semi-infinite n-cladding layer; curve 2 (dotted) represents the more realistic case of a finite (1.0 μm) n-cladding layer. For reference, the maximum Γ_{total} values are also shown for the conventional structure (line 3) and for the conventional structure without the AlGaN layer over the QW's (line 4).

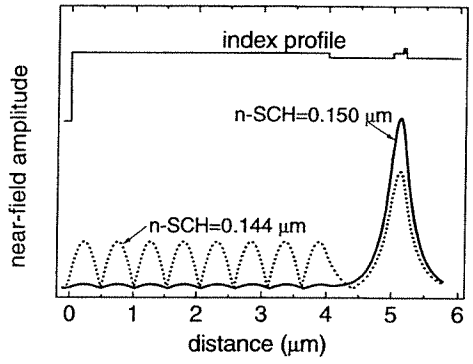

Fig. 6. Transverse near-field amplitude profiles for two asymmetric nitride laser structures. The dashed curve represents the case when the n-waveguide thickness is 0.144 μm, for which resonant outcoupling occurs, resulting in a very low Γ_{total}. The solid curve represents a slightly greater n-waveguide thickness 0.150 μm, which avoids this resonant leakage.

When the total optical confinement factor is calculated assuming a finite n-cladding layer (thickness 1 μm), the values are nearly identical to those computed for a semi-infinite n-cladding, except for several resonances where Γ_{total} becomes very low. This is shown by the dotted curve (no. 2) in Fig. 5. The transverse mode in nitride lasers is essentially a standing wave that occupies the entire epitaxial structure. The mode is largely confined by the intended AlGaN-clad waveguide, but still some light leaks out into the underlying, parasitic waveguide formed by the thick GaN layer. For those narrow bands of n-waveguide thickness where Γ_{total} drops to a very low value, there is no high-order mode which strongly overlaps the MQW active region. Instead, examination of the near-field transverse mode profiles indicates that resonant outcoupling occurs in the vicinity of these Γ_{total} minima. Specifically, the intensity of light propagating in the thick underlying GaN layer becomes very great when the n-waveguide thickness approaches one of these resonant values.

This resonant leakage is illustrated in Fig. 6, where the transverse mode is compared for two representative thicknesses of the n-waveguide in the asymmetric waveguide structure: 0.144 μm, which corresponds to one of the low-Γ_{total} resonances, and 0.150 μm, a slightly greater thickness that avoids

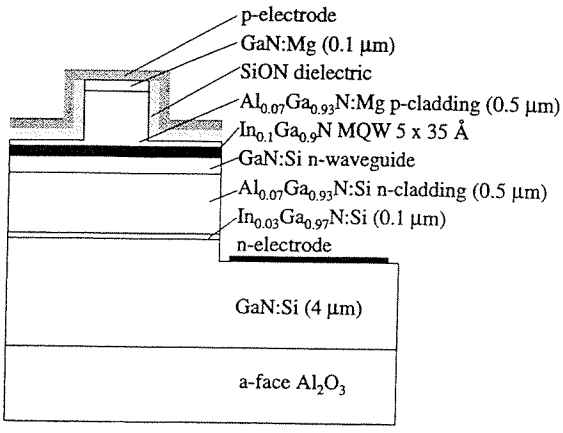

Fig. 7. Ridge-waveguide device structure incorporating asymmetric transverse waveguide.

the resonant outcoupling. Despite the small difference in the waveguide thickness, there is a dramatic change in the transverse mode. Of course, this phenomenon is not unique to the asymmetric waveguide structure; an analogous resonant condition also applies to conventional nitride laser structures. So long as these resonances are avoided, however, the Γ_{total} values are essentially identical for 1-μm and semi-infinite cladding layers. It is also important to note that the n-waveguide thicknesses for which these resonances occur depend upon the wavelength and index values assumed, as well as the MQW and n-cladding layer thicknesses and compositions. Thus, it is apparent from Fig. 5 that, for comparing the optical confinement factors available from specific structures, the semi-infinite cladding layer approximation is accurate. Finally, this resonant outcoupling may be eliminated by depositing nitride laser heterostructures over thick AlGaN (rather than GaN) layers [27]. In this case, if the AlGaN composition is chosen such that its refractive index is lower than the modal effective index, the parasitic waveguide is eliminated and no mode leakage will occur.

IV. Asymmetric Waveguide Nitride Laser Diode

We have verified the viability of the asymmetric waveguide structure by fabricating a nitride laser diode of the design illustrated in Figs. 2 and 4 [28]. The device structure was deposited on an a-face sapphire substrate, as shown schematically in Fig. 7. The MQW layer structure is further summarized in Table I. It is essentially identical to those described by Nakamura *et al.*, except for the asymmetric waveguide structure, in which the $Al_{0.2}Ga_{0.8}N$:Mg layer over the QW's and the GaN:Mg upper waveguide layer are omitted [1]–[10]. Otherwise, the active region contains five 35-Å $In_{0.1}Ga_{0.9}N$ QW's separated by 60-Å $In_{0.02}Ga_{0.98}N$:Si barriers, and the cladding layers are 0.5-μm $Al_{0.07}Ga_{0.93}N$ [19]. Here, the choice of an a-face sapphire substrate is not believed to be significant. In our experience with conventional structures, we have obtained comparable results with a- or c-face substrate wafers. The asymmetric structure was confirmed by transmission electron microscopy and the doping profile by secondary ion mass spectroscopy.

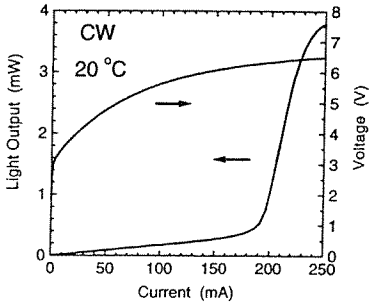

Fig. 8. Light–current and voltage–current characteristics of a 3 μm × 750 μm asymmetric waveguide nitride laser diode for continuous operation.

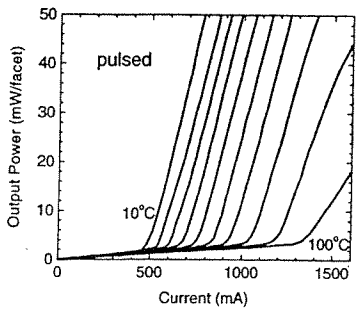

Fig. 10. Light–current characteristics for pulsed operation of a 10 μm × 1000 μm asymmetric waveguide nitride laser diode, at various temperatures.

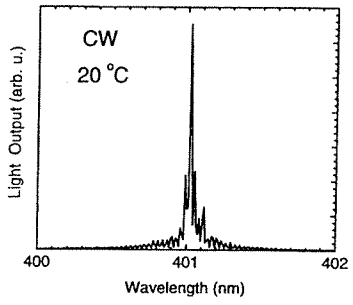

Fig. 9. Emission spectrum of 3 μm × 750 μm asymmetric waveguide nitride laser diode for CW operation at 20 °C.

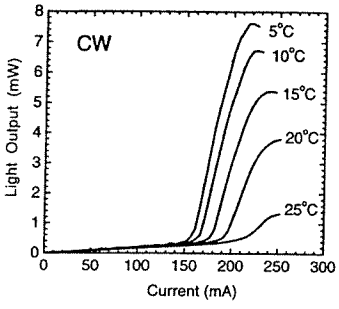

Fig. 11. Light–current characteristics for CW operation of a 3 μm × 750 μm asymmetric waveguide nitride laser diode, at various temperatures.

Lateral waveguiding is accomplished with a 3-μm-wide ridge waveguide. Both the ridge and the laser mirrors were chemically-assisted ion-beam etched (CAIBE) using Ar ions in a blanket mixture of Cl–BCl_3 reactive gas [18]. The laser cavity length was 750 μm, and high-reflection coatings of SiO_2–TiO_2 were evaporated on each mirror in order to minimize the mirror loss for the lowest threshold current. To define the p-contact, an insulating silicon oxy-nitride (SiON) film was first deposited around the ridge. Subsequently, a 2-μm-wide window was etched through the dielectric, along the top of the ridge, to allow the p-electrode to contact the ridge. A lateral n-contact was fabricated by etching through the p-type layers, and depositing an n-electrode on the exposed n-type GaN layer. Finally, for more efficient heat dissipation, the sapphire wafer was thinned to about 100 μm, then indium-soldered p-side-up to a copper heatsink.

The light–current and voltage–current characteristics of the 3 μm × 750 μm nitride laser diode operating continuously at a heat-sink temperature of 20 °C are shown in Fig. 8. The threshold current is about 190 mA, for a threshold current density of 8.4 kA/cm^2. Due to heating, this is considerably higher than the room-temperature pulsed threshold current density, which was 5.2 kA/cm^2. The threshold voltage was about 6.3 V. Light output power greater than 3 mW per facet was obtained, with a differential quantum efficiency of 2.9% per mirror. The emission spectrum was centered at 401 nm, as shown in Fig. 9.

The temperature dependence of the pulsed threshold current is shown for a 10 μm × 1000 μm laser (without mirror coatings) in Fig. 10, for heat-sink temperatures ranging from 10 °C to 100 °C, in 10 °C increments. The threshold current ($I_{\rm th}$) increases roughly exponentially with temperature (T): $I_{\rm th} \propto \exp(T/T_o)$, with a characteristic temperature T_o = 93 K. For comparison, the T_o value for conventional structures we have fabricated is typically 110–115 K. Thus, the threshold current of these asymmetric waveguide laser diodes is more temperature-sensitive than for our own and previously reported conventional layer structures, which had T_o values as high as ~150 K [10]. This might be a result of electron leakage, since the confinement barrier offered by the $Al_{0.07}Ga_{0.93}N$ p-cladding layer of the asymmetric waveguide structure is lower than that available from the $Al_{0.2}Ga_{0.8}N$ barrier of the conventional structure. Alternatively, other factors also influence the characteristic temperature value, such as the distribution of injected carriers, or the basic optoelectronic character of the material (impurities, nonradiative defect states, etc.). In fact, the differential quantum efficiencies exhibited by the *L–I* characteristics in Fig. 10 are relatively constant up to about 80 °C. If an appreciable fraction of injected electrons were leaking away, however, the internal quantum efficiency should drop rapidly with temperature. Thus, these data suggest that electron leakage may not be significant near room temperature in the asymmetric waveguide structure. Nevertheless, electron confinement is still expected to be weaker in this asymmetric waveguide structure, compared to the conventional structure.

The *L–I* characteristics for CW operation between 5 °C and 25 °C are shown in Fig. 11. As a result of heating, the threshold increases very rapidly in this temperature range, so that CW operation is barely achieved at 25 °C. The power output is thermally limited, as evidenced by the strong rollover in the *L–I* characteristics.

A constant-current lifetest was performed for the 3 μm × 750 μm asymmetric waveguide nitride laser, operating at 20 °C. Here, the dc current was kept constant at 201 mA, while the light

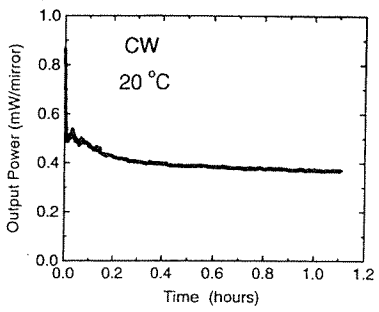

Fig. 12. Constant-current lifetime characteristic of an asymmetric waveguide nitride laser diode.

output was recorded, as shown in Fig. 12. In the first 20–30 s, the light output dropped rapidly from about 0.9 mW/facet to 0.5 mW/facet. This drop is reversible and does not represent degradation of the laser. Instead, it is most likely a result of the temperature equilibrating at a higher value, once current is applied to the device. No sudden failure occurred and laser operation was still observed after 1.1 h (at which point the lifetest was stopped). However, the longer term degradation apparent in Fig. 12 was permanent. The degradation mechanism is still not understood, but there was no significant change in the *V–I* characteristic. When the *L–I* characteristic was remeasured after the 1.1-h lifetest, however, the threshold current had increased, and the differential quantum efficiency had decreased.

While these data demonstrate the viability of the asymmetric waveguide structure, it is still not clear whether this structure offers any advantage over the conventional structure, other than its simplicity. We have, for example, also obtained room-temperature CW operation using conventional structures, with roughly similar threshold currents and lifetimes. Although the optical confinement factor achieved with both structures are comparable, the simpler asymmetric waveguide may represent a compromise for electron confinement. Nevertheless, the threshold and and its temperature sensitivity were still sufficiently good to achieve room-temperature CW operation. Further optimization of these laser structures is still required for making a meaningful comparison.

V. Conclusions

In summary, we have described the design and performance characteristics of an asymmetric waveguide nitride laser diode layer structure that uses the p-cladding layer to confine injected electrons. This structure represents a departure from conventional nitride laser diode structures, where electron confinement is provided by a separate high-aluminum-content AlGaN tunnel barrier layer placed over the MQW active region. Here, the p-cladding layer is instead placed immediately over the MQW, such that the QW's are displaced from the center of the waveguide and the optical mode's peak. This nitride laser structure is based upon the recognition that transverse waveguiding in nitride lasers is relatively weak, making them somewhat insensitive to such a waveguide asymmetry. Thus, the optical confinement factor remains comparably high as for the conventional structure. Room-temperature CW operation was achieved with this structure.

Acknowledgment

The authors gratefully acknowledge technical assistance from E. Taggart, D. Treat, F. Endicott, and S. Ready and the support and encouragement of R. Bringans.

References

[1] S. Nakamura, M. Senoh, S. Nagahama, N. Iwasa, T. Yamada, T. Matsushita, H. Kiyoku, and Y. Sugimoto, "InGaN-based multi-quantum-well-structure laser diodes," *Jpn. J. Appl. Phys.*, vol. 35, pp. L74–L76, 1996.

[2] S. Nakamura, M. Senoh, S. Nagahama, N. Iwasa, T. Yamada, T. Matsushita, Y. Sugimoto, and H. Kiyoku, "Room-temperature continuous-wave operation of InGaN multi-quantum-well-structure laser diodes," *Appl. Phys. Lett.*, vol. 69, pp. 4056–4058, 1996.

[3] S. Nakamura, M. Senoh, S. Nagahama, N. Iwasa, T. Yamada, T. Matsushita, H. Koyoku, and Y. Sugimoto, "Characteristics of InGaN multi-quantum-well-structure laser diodes," *Appl. Phys. Lett.*, vol. 68, pp. 3269–3271, 1996.

[4] S. Nakamura, S. Nagahama, N. Iwasa, T. Yamada, T. Matsushita, Y. Sugimoto, and H. Koyoku, "Room-temperature continuous-wave operation of InGaN multi-quantum-well-structure laser diodes with a long lifetime," *Appl. Phys. Lett.*, vol. 70, pp. 868–870, 1997.

[5] S. Nakamura, "InGaN/GaN/AlGaN-based laser diodes with an estimated lifetime of longer than 10 000 hours," *MRS Bull.*, pp. 37–43, May 1998.

[6] S. Nakamura, M. Senoh, S. Nagamaa, N. Iwasa, T. Yamada, T. Matsushita, H. Kiyoku, Y. Sugimoto, T. Kozaki, H. Umemoto, M. Sano, and K. Chocho, "InGaN/GaN/AlGaN-based laser diodes with modulation-doped strained-layer superlattices grown on an epitaxially laterally overgrown GaN substrate," *Appl. Phys. Lett.*, vol. 72, pp. 211–213, 1998.

[7] ——, "Violet InGaN/GaN/AlGaN-based laser diodes with an output power of 420 mW," *Jpn. J. Appl. Phys.*, vol. 37, pp. L627–L629, 1998.

[8] ——, "High-power, long-lifetime InGaN/GaN/AlGaN-based laser diodes grown on pure GaN substrates," *Jpn. J. Appl. Phys.*, vol. 37, pp. L309–L312, 1998.

[9] S. Nakamura, "High-power InGaN-based blue laser diodes with a long lifetime," *J. Cryst. Growth*, vol. 195, pp. 242–247, 1998.

[10] ——, "InGaN multiquantum-well-structure laser diodes with GaN-AlGaN modulation-doped strained-layer superlattices," *IEEE J. Select. Topics Quantum Electron.*, vol. 4, pp. 483–489, 1998.

[11] A. C. Abare, M. P. Mack, M. Hansen, R. K. Sink, P. Kozodoy, S. Keller, J. S. Speck, J. E. Bowers, U. K. Mishra, L. A. Coldren, and S. P. DenBaars, "Cleaved and etched facet nitride laser diodes," *IEEE J. Select. Topics Quantum Electron.*, vol. 4, pp. 505–509, 1998.

[12] T. Kobayashi, F. Nakamura, K. Naganuma, T. Tojyo, H. Nakajima, T. Asatsuma, H. Kawai, and M. Ikeda, "Room-temperature continuous-wave operation of GaInN/GaN multiquantum well laser diode," *Electron. Lett.*, vol. 34, pp. 1494–1495, 1998.

[13] A. Kuramata, S. Kubota, R. Soejima, K. Domen, K. Horino, and T. Tanahashi, "Room-temperature continuous wave operation of InGaN laser diodes with vertical conducting structure on SiC substrate," *Jpn. J. Appl. Phys.*, vol. 37, pp. L1373–L1375, 1998.

[14] M. Kuramoto, C. Sasaoka, Y. Hisanaga, A. Kimura, A. Yamaguchi, H. Sunakawa, N. Kuroda, M. Nido, A. Usui, and M. Mizuta, "Room-temperature continuous wave operation of InGaN multi-quantum-well laser diodes grown on an n-GaN substrate with a backside n-contact," *Jpn. J. Appl. Phys.*, vol. 38, pp. L184–L186, 1999.

[15] K. Itaya, M. Onomura, J. Nishio, L. Sugiura, M. Suzuki, J. Rennie, S. Nunuoe, M. Yamamoto, H. Fujimoto, Y. Ohba, G. Hatakoshi, and M. Ishikawa, "Room-temperature pulsed operation of nitride based multi-quantum-well laser diodes with cleaved facets on conventional c-face sapphire substrates," *Jpn. J. Appl. Phys.*, vol. 35, pp. L1315–L1317, 1996.

[16] H. Katoh, T. Takeuchi, C. Anbe, R. Mizumoto, S. Yamaguchi, C. Wetzel, H. Amano, I. Akasaki, Y. Kaneko, and N. Yamada, "GaN based laser diode with focused ion beam etched mirrors," *Jpn. J. Appl. Phys.*, vol. 37, pp. L444–L446, 1998.

[17] Y. Kimura, M. Miyachi, H. Takahashi, T. Tanaka, M. Nishitsuka, A. Watanabe, H. Ota, and K. Chijuma, "Room-temperature pulsed operation of GaN-based laser diodes on a-face sapphire substrate grown by low-pressure metalorganic chemical vapor deposition," *Jpn. J. Appl. Phys.*, vol. 37, pp. L1231–L1233, 1998.

[18] M. Kneissl, D. Bour, N. Johnson, L. Romano, B. Krusor, R. Donaldson, J. Walker, and C. Dunnrowicz, "Characterization of AlGaInN diode lasers with mirrors from chemically assisted ion beam etching," *Appl. Phys. Lett.*, vol. 72, pp. 1539–1541, 1998.
[19] D. Bour, M. Kneissl, L. Romano, R. Donaldson, C. Dunnrowicz, N. Johnson, and G. Evans, "Stripe-width dependence of threshold current for gain-guided AlGaInN laser diodes," *Appl. Phys. Lett.*, vol. 74, pp. 404–406, 1999.
[20] S. J. Rosner, E. C. Carr, M. J. Ludowise, G. Girolami, and H. I. Erikson, "Correlation of carthodoluminescince inhomogeneity with microstructural defects in epitaxial GaN grown by metalorganic chemical-vapor deposition," *Appl. Phys. Lett.*, vol. 70, pp. 420–422, 1997.
[21] W. Goetz, private communication.
[22] C. H. Chen, H. Liu, D. Steigerwald, W. Imler, C. P. Kuo, M. G. Craford, M. Ludowise, S. Lester, and J. Amano, "A study of parasitic reactions between NH_3 and TMGa or TMAI," *J. Electron. Mater.*, vol. 25, pp. 1004–1008, 1996.
[23] M. Ishikawa, H. Shiozawa, K. Itaya, G. Hatakoshi, and Y. Uematsu, "Temperature dependence of the threshold current for InGaAlP visible laser diodes," *IEEE J. Quantum Electron.*, vol. 27, pp. 23–29, 1991.
[24] S. A. Wood, P. M. Smowton, C. H. Molloy, P. Blood, D. J. Somerford, and C. C. Button, "Direct monitoring of thermally activated leakage current in AlGaInP laser diodes," *Appl. Phys. Lett.*, vol. 74, pp. 2540–2542, 1999.
[25] D. P. Bour, D. W. Treat, R. L. Thornton, R. S. Geels, and D. F. Welch, "Drift leakage current in AlGaInP quantum-well lasers," *IEEE J. Quantum Electron.*, vol. 29, pp. 1337–1343, 1993.
[26] D. Hofstetter, D. P. Bour, R. L. Thornton, and N. M. Johnson, "Excitation of a higher order transverse mode in an optically pumped InGaN multiquantum well laser structure," *Appl. Phys. Lett.*, vol. 70, pp. 1650–1652, 1997.
[27] T. Takeuchi, T. Detchprohm, M. Iwaya, N. Hayashi, K. Isomura, K. Kimura, M. Yamaguchi, H. Amano, I. Akasaki, Yw. Kaneko, R. Shioda, S. Watanabe, T. Hidaka, Y. Yamaoka, Ys. Kaneko, and N. Yamada, "Improvement of far-field pattern in nitride laser diodes," *Appl. Phys. Lett.*, vol. 75, 1999.
[28] M. Kneissl, D. P. Bour, C. G. Van de Walle, L. T. Romano, J. E. Northrup, R. M. Wood, M. Teepe, and N. M. Johnson, "Room temperature, continuous-wave operation of InGaN multiple quantum well laser diodes with an asymmetric waveguide structure," *Appl. Phys. Lett.*, vol. 75, pp. 581–583, 1999.

D. P. Bour, photograph and biography not available at the time of publication.

M. Kneissl, photograph and biography not available at the time of publication.

C. G. Van de Walle, photograph and biography not available at the time of publication.

G. A. Evans, photograph and biography not available at the time of publication.

L. T. Romano, photograph and biography not available at the time of publication.

J. Northrup, photograph and biography not available at the time of publication.

M. Teepe, photograph and biography not available at the time of publication.

R. Wood, photograph and biography not available at the time of publication.

T. Schmidt, photograph and biography not available at the time of publication.

S. Schoffberger, photograph and biography not available at the time of publication.

N. M. Johnson, photograph and biography not available at the time of publication.